Inorg. Chem. **2004**, *43*, 5237–5244

On the Mechanism of Dioxygen Formation from a Di-μ-Oxo-Bridged Manganese Dinuclear Complex

Simon Petrie and Robert Stranger*

Department of Chemistry, The Faculties, The Australian National University, Canberra ACT 0200, Australia

Received January 6, 2004

Density functional theory (DFT) calculations, using the Becke–Perdew gradient-corrected functional with a triple-ζ-plus-polarization basis set, have been used to characterize the $[(H_2O)(H_3N)_3Mn(\mu\text{-}O)_2Mn(NH_3)_3(OH_2)]^{q+}$ (q = 2–5) complexes. This structure has been proposed as a possible model for the oxygen-releasing site of the photosystem II (PSII) reaction center. We have performed full optimizations to locate stationary points in various spin states for each of the +2 to +5 charge states. Our calculations indicate that O_2 release from the vacuum-phase +5 charge state complex is barrier inhibited, in contrast to the results of a recent DFT study. We report several new di-μ-oxo-bridged stationary points with spin multiplicities of $S = {}^1/_2$, ${}^3/_2$, and ${}^5/_2$ and effective metal oxidation states of $Mn^{IV}Mn^{V}$ for the +5 charge state. Finally, calculations employing the 'conductorlike screening model' (COSMO), to address the inclusion of solvent effects, indicate that dissociative O_2 release from the +5 charge state model complex is inhibited by a major barrier and is therefore apparently highly disfavored.

Introduction

A full understanding of the structure and operation of the tetranuclear manganese cluster that is believed to form the core of the photosystem II (PSII) reaction center[1−4] remains elusive despite an intensive concentration of research resources. This camera-shy manganese-containing structure, which to date is best characterized by a series of 3.5−3.8-Å-resolution crystal structures of the PSII enzyme,[5−7] is regarded as crucial to the photosynthetic process.

$$2H_2O + h\nu \rightarrow O_2 + 4e + 4H^+ \qquad (1)$$

Several models have been proposed for the active site, involving Mn atoms variously bridged by oxo, peroxo, hydroxo, carboxylato, and bicarbonato groups, and with overall metal core configurations ranging from linear to branched to cubanelike structures.[8−13] It is believed that four distinct photooxidation steps are involved in the conversion of the lowest (S_0) to the highest, oxygen-evolving (S_4) oxidation states, with O_2 loss being accompanied by the spontaneous regeneration of the S_0 state. One of the many models to have been presented for the active site (in which only two of the four Mn atoms may be sensitive to photooxidation) is the di-μ-oxo bridged species (**I**),[14]

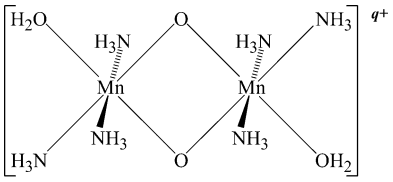

(**I**)

which, with both Mn atoms in identical oxidation states, is expected to adopt C_{2h} symmetry. A recent study (hereafter

* Author to whom correspondence should be addressed. E-mail: rob.stranger@anu.edu.au.

(1) Ananyev, G. M.; Zaltsman, L.; Vasko, C.; Dismukes, G. C. *Biochim. Biophys. Acta* **2001**, *1503*, 52.
(2) Goussias, C.; Boussac, A.; Rutherford, A. W. *Philos. Trans. R. Soc. London, Ser. B* **2002**, *357*, 1369.
(3) Yachandra, V. K. *Philos. Trans. R. Soc. London, Ser. B* **2002**, *357*, 1347.
(4) Barber, J. *Q. Rev. Biophys.* **2003**, *36*, 71.
(5) Zouni, A.; Witt, H.-T.; Kern, J.; Fromme, P.; Krauss, N.; Saenger, W.; Orth, P. *Nature* **2001**, *409*, 739.
(6) Kamiya, N.; Shen, J.-R. *Proc. Natl. Acad. Sci. Acad. U.S.A.* **2003**, *100*, 98.
(7) Ferreira, K. N.; Iverson, T. M.; Maghlaoui, K.; Barber, J.; Iwata, S. *Science* **2004**, *303*, 1831.
(8) Peloquin, J. M.; Campbell, K. A.; Randall, D. W.; Evanchik, M. A.; Pecoraro, V. L.; Armstrong, W. H.; Britt, R. D. *J. Am. Chem. Soc.* **2000**, *122*, 10926.
(9) Robblee, J. H.; Cinco, R. M.; Yachandra, V. K. *Biochim. Biophys. Acta* **2001**, *1503*, 7.
(10) Vrettos, J. S.; Limburg, J.; Brudvig, G. W. *Biochim. Biophys. Acta* **2001**, *1503*, 229.
(11) Carrell, T. G.; Tyryshkin, A. M.; Dismukes, G. C. *J. Biol. Inorg. Chem.* **2002**, *7*, 2.

10.1021/ic049967k CCC: $27.50
Published on Web 07/24/2004

abbreviated as ARA)[14] employing the B3-LYP hybrid density functional method and the LANLDZ double-ζ basis set has promoted the hypothesis that O_2 release from this complex becomes spontaneous upon its oxidation to the +5 charge state overall. In response to the current widespread and intensive interest in the exact mechanism of action within PSII, we have conducted our own DFT evaluation of the structural and electronic response of compound **I** to repeated oxidation. The research presented here has used a polarization-augmented triple-ζ basis set throughout, with particular care given to the limitations of C_{2h} symmetry in describing the Mn^{III}/Mn^{IV} and Mn^{IV}/Mn^{V} oxidation state combinations, as well as the question of stability or instability of the +5 charge state dinuclear complex within both the gas and condensed phases.

Computational Details

All calculations described in this work were variously performed on Linux-based Pentium IV 1.7−2.0-GHz computers or on four-processor nodes of the AlphaServer SC supercomputer housed at the ANU Supercomputing Facility, using the Amsterdam Density Functional (ADF) program, version ADF2002,[15] developed by Baerends et al.[16] Calculations used the Vosko−Wilk−Nusair (VWN)[17] parametrization of the electron gas in the local density approximation (LDA) combined with the gradient-corrected functionals of Becke and Perdew (BP).[18,19] An evaluation of the performance for several pure density functionals, via prediction of the bond lengths within first-transition-row metallocenes,[20] has found BP to be among the most reliable functionals with regard to the characterization of molecular geometries. The TZP (triple-ζ-plus-polarization) basis sets, featuring Slater-type orbitals, were used for all atoms. Electrons in orbitals up to and including 1s {N, O} or 2p {Mn} were treated in accordance with the frozen-core approximation. Optimized geometries were obtained using the gradient algorithm of Versluis and Ziegler.[21] Solvent field calculations were performed using the conductorlike screening model (COSMO)[22−24] as implemented within the ADF program suite,[25] with dielectric constant (ϵ) values of 4.0, 10.0, and 78.4 used in conjunction with the default settings for other solvent-field parameters. Calculations on low overall spin states ($S = 0, {}^1/_2, 1$) also routinely employed the broken-symmetry technique (BS),[26,27] which introduces an asymmetry in the initial spin densities on two otherwise symmetry-related atoms (in the present cases, the Mn or bridging O atoms). The utility of the BS approach to computational problems of ferromagnetic versus antiferromagnetic coupling has been reviewed by Ruiz et al.[28]

Results and Discussion

1. Structural and Electronic Properties of the Optimized Stationary Points. We have characterized several apparent minima for each of the +2 to +5 overall charge states of the dinuclear complexes, which correspond to Mn oxidation states Mn^{III}/Mn^{III}, Mn^{III}/Mn^{IV}, Mn^{IV}/Mn^{IV}, and Mn^{IV}/Mn^{V} assuming an oxidation number of −2 on each of the bridging oxygen atoms. These stationary points were variously obtained within the geometric constraints of C_{2h} or C_s symmetry. Additionally, when C_{2h} geometry was employed, relaxation of the electronic configuration was explored to permit C_s-symmetry descriptions of the molecule's electronic state, such as the broken-symmetry solution for weakly antiferromagnetically coupled species. The resulting stationary points are summarized in Table 1, which also includes, for purposes of comparison, the calculated relative energies obtained in the ARA study[14] as well as the experimentally observed ranges of Mn−Mn, Mn−O, and O−O bond lengths reported for representative Mn dinuclear complexes. The latter values are also taken from ARA,[14] on the basis of data contained within the Cambridge Structural Database.

We stress that the model structure considered here (and by ARA)[14] is necessarily somewhat simplistic and cannot be expected to represent the complexity that likely resides within the true PSII active site reliably. Nontheless, rigorous evaluation of such models is an important effort in seeking to understand the detailed mechanism of PSII, and to this end, it remains useful to determine in what respects the model succeeds or fails in replicating the dioxygen-releasing properties of the PSII active site.

There are many points of substantial agreement between our own results and the B3-LYP/LANLDZ calculations of the ARA study. For example, ARA[14] noted that the O−O distance (between the two oxo bridge atoms), in all of the stationary points from the +2 to +4 charge state overall, is invariably longer than 2.28 Å, indicating an absence of O−O bonding. Our own geometry optimizations reveal that at the BP/TZP level of theory the shortest O−O distance within the +2 to +4 charge states is found in the broken-symmetry ($M_S = 0$) $Mn^{IV}Mn^{IV}$ complex, for which our O−O separation of 2.272 Å is in excellent agreement with the ARA[14] value of 2.283 Å. Both studies also verify that the complexes featuring Mn^{III} preferentially adopt high-spin rather than low-spin electronic configurations on the individual Mn atoms.

(12) Robblee, J. H.; Messinger, J.; Cinco, R. M.; McFarlane, K. L.; Fernandez, C.; Pizarro, S. A.; Sauer, K.; Yachandra, V. K. *J. Am. Chem. Soc.* **2002**, *124*, 7459.
(13) Visser, H.; Dube, C. E.; Armstrong, W. H.; Sauer, K.; Yachandra, V. K. *J. Am. Chem. Soc.* **2002**, *124*, 11008.
(14) Aullón, G.; Ruiz, E.; Alvarez, S. *Chem.—Eur. J.* **2002**, *8*, 2508.
(15) Baerends, E. J.; Bérces, A.; Bo, C.; Boerrigter, P. M.; Cavallo, L.; Deng, L.; Dickson, R. M.; Ellis, D. E.; Fan, L.; Fischer, T. H.; Fonseca Guerra, C.; van Gisbergen, S. J. A.; Groeneveld, J. A.; Gritsenko, O. V.; Harris, F. E.; van den Hoek, P.; Jacobsen, H.; van Kessel, G.; Kootstra, F.; van Lenthe, E.; Osinga, V. P.; Philipsen, P. H. T.; Post, D.; Pye, C.; Ravenek, W.; Ros, P.; Schipper, P. R. T.; Schreckenbach, G.; Snijders, J. G.; Sola, M.; Swerhone, D.; te Velde, G.; Vernooijs, P.; Versluis, L.; Visser, O.; van Wezenbeek, E.; Wiesenekker, G.; Wolff, S. K.; Woo, T. K.; Ziegler, T. *ADF2002.03*; S. C. M.: Vrije Universiteit, Theoretical Chemistry: Amsterdam, 2002.
(16) Velde, G. T.; Bickelhaupt, F. M.; Baerends, E. J.; Guerra, C. F.; van Gisbergen, S. J. A.; Snijders, J. G.; Ziegler, T. *J. Comput. Chem.* **2001**, *22*, 931.
(17) Vosko, S. H.; Wilk, L.; Nusair, M. *Can. J. Phys.* **1980**, *58*, 1200.
(18) Becke, A. D. *Phys. Rev. A* **1988**, *38*, 3098.
(19) Perdew, J. P. *Phys. Rev. B* **1986**, *33*, 8822.
(20) Swart, M.; Snijders, J. G. *Theor. Chem. Acc.* **2003**, *110*, 34.
(21) Versluis, L.; Ziegler, T. J. *J. Chem. Phys.* **1988**, *88*, 322.
(22) Pascual-Ahuir, J. L.; Silla, E.; Tomasi, J.; Bonaccorsi, R. *J. Comput. Chem.* **1987**, *8*, 778.
(23) Klamt, A.; Schüürmann, G. *J. Chem. Soc., Perkin Trans. 2* **1993**, 799.
(24) Klamt, A. *J. Phys. Chem.* **1995**, *99*, 2224.
(25) Pye, C. C.; Ziegler, T. *Theor. Chem. Acc.* **1999**, *101*, 396.
(26) Noodleman, L.; Norman, J. G., Jr. *J. Chem. Phys.* **1979**, *70*, 4903.
(27) Noodleman, L. *J. Chem. Phys.* **1981**, *74*, 5737.
(28) Ruiz, E.; Cano, J.; Alvarez, S.; Alemany, P. *J. Comput. Chem.* **1999**, *20*, 1391.

Table 1. Key Energetic and Geometric Parameters Obtained for Various Charge States and Spin States of $[Mn_2(\mu\text{-}O)_2(H_2O)_2(NH_3)_6]^{n+}$ from Calculations Employing the Becke−Perdew Density Functional Approach

				distances/Å			E_{rel}/kJ mol^{-1}		μ_{spin} (Mn/O)			
charge state	spin state	symm	E_{tot}/eV	Mn−Mn	O−O	Mn−O	this work	ARA	Mn_A	Mn_B	μ-O_A	μ-O_B
2+ (III, III)	BS	C_{2h}[a−c]	−166.399	2.690	2.465	1.797, 1.851	−98		3.74	−3.74	0.03	−0.03
	$S = 4$	C_{2h}[a,d]	−166.060	2.729	2.485	1.815, 1.875	−65		3.88	3.88	0.13	0.13
	BS	C_s[e]	−165.855	2.710	2.463	1.792−1.872	−46		3.74	−3.71	0.01	−0.01
	$S = 4$	C_s[e]	−165.520	2.754	2.484	1.817−1.898	−13		3.88	3.85	0.15	0.10
	BS	C_{2h}[b,c]	−165.384	2.710	2.441	1.804, 1.843	0	0	3.70	−3.70	−0.01	0.01
	$S = 4$	C_{2h}[d]	−165.028	2.747	2.474	1.831, 1.866	34	21	3.85	3.85	0.11	0.11
	$S = 2$	C_s[e]	−164.652	2.673	2.525	1.834−1.844	71		3.71	0.12	0.08	0.07
	$S = 2$	C_{2h}[a,d]	−164.512	2.652	2.442	1.756, 1.848	84[a]		2.01	2.01	0.06	0.06
	$S = 2$	C_{2h}[d]	−164.027	2.756	2.438	1.785, 1.893	131	176	1.84	1.84	0.21	0.21
	expt			**2.67−2.70**	**2.50−2.53**	**1.83−1.85**						
3+ (III, IV)	$S = 1/2$	C_s[e]	−153.300	2.761	2.353	1.773−1.864	−74		3.79	−2.55	−0.14	−0.19
	$S = 7/2$	C_s[e]	−152.971	2.747	2.437	1.780−1.917	−43		3.95	2.80	0.15	0.20
	$S = 1/2$	C_s	−152.745	2.766	2.360	1.769−1.877	−21		3.73	−2.51	−0.15	−0.19
	$S = 1/2$	C_{2h}[b]	−152.528	2.762	2.345	1.804, 1.820	0	0	3.43	−2.34	−0.08	−0.13
	$S = 7/2$	C_{2h}[d]	−152.280	2.748	2.446	1.805, 1.873	24	21	3.42	3.42	0.13	0.13
	$S = 1/2$	C_{2h}	−151.206	2.764	2.308	1.754, 1.846	128		0.65	0.65	−0.11	−0.11
	expt			**2.55−2.74**		**1.77−1.89**						
4+ (IV, IV)	BS	C_{2h}[c,d]	−135.197	2.834	2.272	1.789, 1.842	0	0	2.77	−2.77	−0.02	0.02
	$S = 3$	C_{2h}[e]	−134.904	2.806	2.371	1.805, 1.868	28	14	2.96	2.96	0.17	0.17
	expt			**2.57−2.78**	**2.25−2.54**	**1.77−1.83**						
5+ (IV, V)	$S = 5/2$	C_s	−111.496	2.888	2.304	1.764−1.930	0		2.80	2.83	−0.10	−0.10
	$S = 5/2$	C_{2h}	−111.465	2.921	2.312	1.748, 1.971	3		2.81	2.81	−0.09	−0.09
	$S = 1/2$	C_s	−111.456	2.945	2.271	1.682−2.096	4		3.01	−1.95	0.02	−0.11
	$S = 1/2$	C_{2h}[c]	−111.266	2.925	2.272	1.722, 1.973	22		2.85	−1.87	0.07	−0.07
	$S = 1/2$	C_{2h}[c,d]	−111.223	3.213	2.020	1.829, 1.964	26		2.90	−2.93	0.46	0.44
	$S = 3/2$	C_s	−110.896	2.932	2.240	1.714−1.990	58		3.06	0.18	−0.14	0.03
	$S = 3/2$	C_{2h}[f]	−110.832	2.852	2.302	1.698, 1.958	64		1.81	1.81	−0.15	−0.15
	$S = 1/2$	C_{2h}	−110.234	2.871	2.316	1.676, 1.999	122		0.45	0.45	0.13	0.13
	$S = 7/2$	C_{2h}	dissoc[g]									
	$S = 7/2$	C_s	dissoc[g]									

[a] This optimized geometry possessed the two H_2O ligands in a loosely bound configuration (each formally bound to two NH_3 ligands rather than to Mn). [b] The results identified here are for a geometry optimization in C_{2h} symmetry, but with a wave function possessing C_s symmetry. [c] Identical results were obtained when geometric symmetry was relaxed from C_{2h} to C_s. [d] Identical results were obtained when geometric and electronic symmetry were relaxed from C_{2h} to C_s. [e] This optimized geometry possessed one H_2O ligand in a loosely bound configuration, formally coordinated to two NH_3 ligands. [f] Identical results were obtained when electronic symmetry was relaxed from C_{2h} to C_s. [g] Within this spin state, dissociation resulted from all starting geometries used; no $S = 7/2$ local minimum could be obtained on the +5 charge state surface.

The +2 to +4 charge state complexes also exhibit a consistent preference for antiferromagnetic coupling between Mn atoms, although the energy of the high-spin $S = 10 - n/2$ (n = overall charge state) above the broken-symmetry $M_S = 0$ or $S = 1/2$ configuration is always somewhat greater in our calculations than in the results of the earlier study. This tendency likely reflects the systematic difference in the treatment of singlet/triplet splittings by the Becke−Perdew pure density functional[18,19] in the present work versus the hybrid B3-LYP functional[29,30] used by ARA.[14] It is quite well established[28] that pure DFT methods incorporating the Becke exchange functional, such as Becke−Perdew, are prone to overestimate the total energy of high-spin states. Conversely, the evaluation of the performance of B3-LYP on this issue indicates a tendency to stabilize high-spin states artificially.[31] It is thus reasonable to suggest that the true high-spin/low-spin splittings for the +2 to +4 charge state species most probably lie between our values and those of ARA. Only the +5 charge state, accessible through our calculations but problematic in ARA,[14] shows ferromagnetic coupling to be slightly favored over an antiferromagnetic interaction. For this charge state, the $S = 5/2$ spin-state structure is marginally lower in energy than the $S = 1/2$ (antiferromagnetic) minimum.

A more detailed perusal of the calculated interatomic distances reveals some significant differences between our BP/TZP results and the B3-LYP/LANLDZ geometries of the ARA study.[14] We have previously remarked that the optimized distance between metal atoms in a bridged dinuclear complex is often particularly sensitive to the theoretical method employed,[32,33] and it is noteworthy that for the stationary points common to the two studies (many of our C_s-symmetry stationary points are not featured in ARA)[14] the Mn−O[34] and O−O distances show reasonable agreement with experiment but the calculated Mn−Mn distances are consistently larger than the upper limit of the experimental range. Our contention is that the optimized structures of these vacuum-phase complexes are sensitive to the influence of

(29) Becke, A. D. *J. Chem. Phys.* **1993**, *98*, 5648.
(30) Lee, C.; Yang, W.; Parr, R. G. *Phys. Rev. B* **1988**, *37*, 785.
(31) Salomon, O.; Reiher, M.; Hess, B. A. *J. Chem. Phys.* **2002**, *117*, 4729.
(32) McGrady, J. E.; Stranger, R.; Lovell, T. *J. Phys. Chem. A* **1997**, *101*, 6265.
(33) Petrie, S.; Stranger, R. *Inorg. Chem.* **2004**, *43*, 2597.
(34) Note that ARA[14] report only one value in each instance for the Mn−O distances in $Mn^{III}Mn^{III}$ and $Mn^{IV}Mn^{IV}$ stationary points; our own calculations, in both C_{2h} and C_s symmetry, clearly show that the bridging Mn−O trans to the terminal H_2O on the same Mn atom is invariably longer, by up to 0.1 Å, than the other bridging Mn−O distance for the same metal atom.

Coulombic distortion, which, within the crystalline environment, is mitigated by counterion effects. Because the intermetallic interaction is generally that with the greatest degree of flexibility and also because the metal atoms are the principal positive charge centers within the dinuclear complex, the elongation of the metal−metal axis is an almost unavoidable consequence of the lack of stabilizing counterions in the multiply charged structures on which the geometry optimization calculations are performed.[33] In this context, it should be noted that our BP/TZP optimized Mn−Mn distances for the $Mn^{III}Mn^{III}$, $Mn^{III}Mn^{IV}$, and $Mn^{IV}Mn^{IV}$ complexes are always within 0.06 Å of the experimental upper limit for di-μ-oxo bridged Mn complexes with the same metal oxidation state combination, whereas the B3-LYP/LANLDZ optimized values[14] are 0.09−0.11 Å ($Mn^{III}Mn^{III}$), 0.10 Å ($Mn^{III}Mn^{IV}$), and 0.12−0.16 Å ($Mn^{IV}Mn^{IV}$) beyond the reported experimental range. This minor, but nonetheless consistent, difference in bond length estimation by BP/TZP versus B3-LYP/LANLDZ may therefore reflect a propensity of the latter method to underestimate the strength of the condensed-phase Mn−Mn interaction.

The identified tendency of B3-LYP/LANLDZ for Mn−Mn elongation, which may well accurately represent the geometry of the polycharged dinuclear complex in the gas or vacuum phase, is nonetheless problematic because it has a direct influence on the question of the complex's stability as a function of increasing charge state. This is amply demonstrated by the observation that for the +5 overall charge state (corresponding to a $Mn^{IV}Mn^{V}$ complex) no stationary point corresponding to an intact dinuclear complex could be obtained at the B3-LYP/LANLDZ level of theory,[14] whereas we have successfully characterized several such stationary points in various spin states and with either C_s or C_{2h} geometric symmetry imposed. The ARA study[14] concluded that "the Mn^{V} oxidation state cannot be attained within a Mn_2O_2 ring" and implied that oxidation to the +5 charge state produced a complex of $Mn^{IV}Mn^{IV}$ with an O_2^{3-} bridge. In our own calculations, we have found that the $S = {}^1/_2$ and ${}^5/_2$ spin states, which would be expected from antiferromagnetic or ferromagnetic coupling of Mn^{IV} and Mn^{V}, dominate the lowest-energy +5 charge state stationary points (and moreover lack any significant development of spin density on either bridging oxygen atom, contrary to expectations for an O_2^{3-} bridge). In contrast, the $S = {}^7/_2$ spin state, corresponding to a ferromagnetic coupling of Mn^{IV}, Mn^{IV}, and O_2^{3-}, does not appear to possess any viable dinuclear geometries in either C_{2h} or C_s symmetry.

It is pertinent to ask why the $S = {}^1/_2$, ${}^3/_2$, and ${}^5/_2$ spin-state surfaces support local minima in which the dinuclear unit is intact at our BP/TZP level of theory but not at the B3-LYP/LANLDZ level of theory employed in the ARA study.[14] We hypothesize that this is likely a consequence both of the different functionals (BP versus B3-LYP) and of the different basis set sizes (triple-ζ plus polarization versus double-ζ). Although the effect of switching functionals cannot be asssessed using ADF[15] (because this code does not feature hybrid functionals such as B3-LYP), we have performed test calculations to gauge the influence of basis set size. For the C_s-symmetry $S = {}^1/_2$ and ${}^5/_2$ minima on the +5 charge state surface, optimization using the ADF DZ (double-ζ) basis set yielded geometries in which the most significant divergence from the TZP-optimized structures (Table 1) was the extension of the Mn−Mn separation by 0.10 Å in both instances. We interpret this to suggest that these minima are less resistant to Coulombic stress in calculations with a more modest basis set. The trend in +5 charge state Mn−Mn distances (increasing separation with smaller basis set size) is qualitatively consistent with the trend in Mn−Mn separations seen for those +2, +3, and +4 charge state species common to both the present work and the ARA study.[14]

We have also attempted to verify the status of the C_s symmetry $S = {}^1/_2$ and ${}^5/_2$ stationary points as minima by performing vibrational frequency calculations on these geometries. These calculations in fact showed two imaginary vibrational frequencies for each of the input geometries; however, the magnitude of these imaginary frequencies was low ($n_i \approx 100$ cm^{-1}) in each instance, and these rotational modes were found to be associated with the torsional motion of the ammonia H atoms. We interpret the frequency results to indicate that the true $S = {}^1/_2$ and ${}^5/_2$ minima may lack C_s symmetry: further investigation of this issue is likely to prove extremely time-consuming because on the computational platforms used here the characterization of vibrational frequencies (even with retention of C_s symmetry) required calculations of several weeks' duration each.

Note that our location of several stationary points upon the +5 charge state surface does not, in itself, discount the mechanism of spontaneous complex dissociation and O_2 release. Photoionization of the +4 charge state can be considered to be a vertical process, which may initially deposit the nascent +5 charged complex upon a region of the potential energy surface in which fragmentation is then spontaneous. To evaluate this possibility critically, we have performed a more detailed study of the +5 charge state surface as described in the following section.

2. Linear Transits. The ARA study[14] used a rigid model system to investigate the electronic and energetic trends associated with spontaneous O_2 release from $[(H_2O)(H_3N)_3Mn(\mu\text{-}O)_2Mn(NH_3)_3(OH_2)]^{5+}$. In their calculations, the geometry, aside from the central Mn_2O_2 bridge, was frozen at the values optimized for the BS +4 charge state complex; Mn−O was constrained, and the O−O distance was systematically varied from 2.3 to 1.1 Å. They reported the identification of a deep well, at Mn−O = 3.0 Å and O−O $\approx$ 1.3 Å, which they identified as a transient Mn^{II}/Mn^{III} couple connected via a loose molecular dioxygen bridge. In an effort to replicate these results (but concerned over some of the finer points of geometry distortion that appear to result from the constraints used in the earlier study), we performed similar calculations on the ($S = {}^1/_2$) +5 charge state using BP/TZP with fixed Mn−Mn distances and variation of the O−O separation. In keeping with the B3-LYP/LANLDZ results,[14] we found that weakening the Mn−Mn interaction through elongation did indeed result in the adoption of a shorter O−O distance (Figure 1); at r(Mn−Mn) = 5.0 Å, the lowest energy among the sequence of frozen geometries

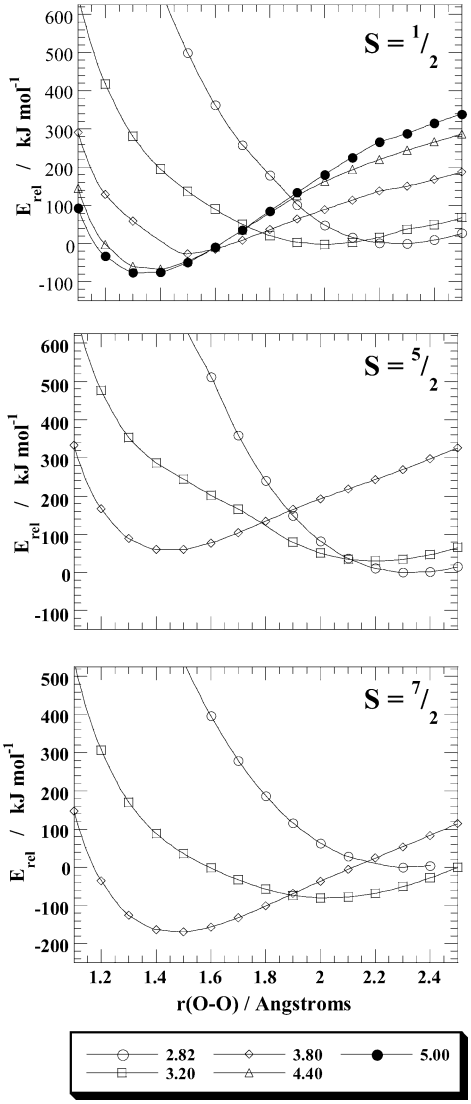

Figure 1. Rigid potential energy scans for the $S = {}^1/_2$, ${}^5/_2$, and ${}^7/_2$ spin states of the +5 charge state complex. The $S = {}^1/_2$ geometric parameters, except for the Mn−Mn and O−O distances, were kept fixed at the values optimized for the BS +4 charge state complex, whereas analogous parameters for the $S = {}^5/_2$ and ${}^7/_2$ scans were fixed at the $S = 3$ +4 charge state optimized values. Each graph depicts the energetic dependence on the O−O separation, whereas the Mn−Mn distance is constrained according to the value shown in the legend. Energies within each scan are expressed relative to the O−O separation local minimum found at the (+4 charge state-optimized) Mn−Mn distance of 2.81 or 2.82 Å.

was found at r(O−O) ≈ 1.3 Å. However, our BP/TZP calculations found a comparatively modest energy difference of ∼ 80 kJ mol^{-1} between the "minimum" with a large O−O separation at the (+4 charge state optimized) Mn−Mn distance of 2.82 Å and the "minimum" with a short O−O separation at r(Mn−Mn) = 5.0 Å, whereas the B3-LYP/LANLDZ calculations[14] suggest a much greater energy release (∼400 kJ mol^{-1}) upon Mn−Mn elongation over a similar distance range. A similar trend, for contraction of the optimum O−O distance with increasing Mn−Mn separation, was also apparent in additional calculations on the $S = {}^5/_2$ and ${}^7/_2$ spin states (Figure 1).

Rigid potential energy scans, such as the examples discussed above, can give an erroneous indication of the energetic factors associated with dissociation. Many of the complex's geometric parameters are constrained at constant values, whereas the Mn−Mn or Mn−O distance is incrementally increased, thus effectively denying the complex substantial opportunity for relaxation through the modes so constrained. To address this concern, we have performed a more relaxed series of linear transit calculations in which the Mn−Mn distance is again incrementally increased while permitting other bond lengths, bond angles, and dihedral angles to be optimized within the overall constraint of C_{2h} symmetry.

The two lowest-energy configurations found for the $Mn^{IV}Mn^{IV}$ +4 charge state complex are BS ($M_S = 0$) and $S = 3$. Therefore, dissociation of a +5 charge state via the one-electron oxidation of the +4 complex should initially involve the $S = {}^1/_2$ or ${}^5/_2$ spin states, which are generated by the removal of a valence d electron from Mn^{IV} or the same spin states, and $S = {}^7/_2$, which are formally accessible by oxidation of an O^{2-} bridge atom.[14] In the relaxed potential energy scans, which we have performed, there are numerous problems associated with changing electronic occupation as the Mn−Mn distance is varied. These changes in occupation, which are identified as avoided crossings in the ARA study,[14] produce discontinuities on the potential energy surface (Figure 2). The data depicted for the $S = {}^1/_2$ spin state demonstrates that in the vacuum phase there is undeniably a considerable driving force toward Mn−Mn separation, with the r(Mn−Mn) = 6.6 Å partially optimized geometry almost 300 kJ mol^{-1} lower in energy than the local minimum at r(Mn−Mn) = 2.8 Å. This dramatic reduction in total energy can be attributed to the Coulombic relaxation with increased separation of the two Mn charge centers. Nevertheless, there is a distinct activation-energy barrier (of ∼10 kJ mol^{-1}) to dissociation. Potential energy curves for the $S = {}^3/_2$ and ${}^5/_2$ spin states show a broadly similar topography, with low barriers to highly exothermic dissociation. The modest barrier height in our BP/TZP calculations suggests that within the vacuum phase the +5 charge state stationary points identified in Table 1 have, at best, a tenuous existence, and it is therefore not surprising that the ARA study,[14] employing a different DFT method and a smaller basis set, did not locate any minima on the +5 charge-state surface.

3. Calculations Incorporating Dielectric Field Corrections. It is well known that calculations on small, highly charged species can be difficult to interpret, insofar as the severe destabilizing influence of Coulombic repulsion on species in vacuum-phase ab initio or DFT calculations does not accurately reflect the much milder influence of Coulombic effects within condensed-phase environments.

In the B3-LYP/LANLDZ study,[14] considerable weight was placed upon the putative stabilization of the nominal $Mn^{III}Mn^{III}(O_2^{-})$ structure compared to the $Mn^{IV}Mn^{IV}(O_2^{3-})$ species of the same overall +5 charge state. As represented by single-point calculations with, respectively, {r(Mn−O) = 2.50 Å, r(O−O) = 1.42 Å} and {r(Mn−O) = 1.85 Å, r(O−O) = 1.99 Å}, ARA found the (O_2^{-})-bridged species to be approximately 300 kJ mol^{-1} lower in energy than the (O_2^{3-})-bridged configuration. This relative ordering was maintained in calculations incorporating a dielectric environ-

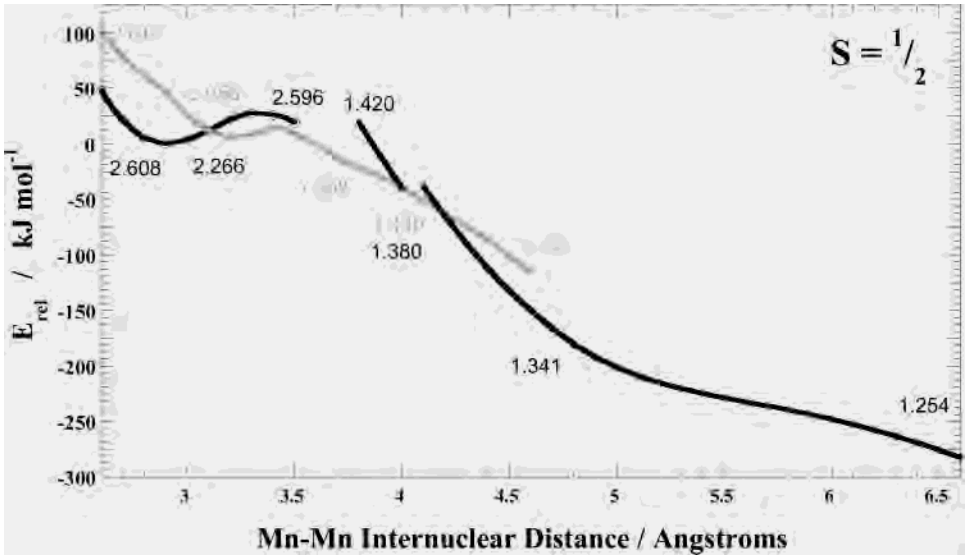

Figure 2. Relaxed, vacuum-phase ($\epsilon = 1$) potential energy scan for the $S = {}^1/_2$ spin state of the +5 charge state complex. Discontinuities in the curves represent avoided crossings between different electronic states of the same spin multiplicity, consistent with differing occupations of the molecular orbitals derived from Mn valence d and 2(s,p) μ-oxo bridge atoms. Curves shown in black and half-tone highlight different states having different O−O bridging distances (identified, in angstroms, as the numbers associated with various partially optimized geometries along the PE curves) at the same Mn−Mn distance.

Table 2. Assessment of Solvent Effects for Key Charge States and Spin States of $[Mn_2(\mu\text{-}O)_2(H_2O)_2(NH_3)_6]^{n+}$, from COSMO Calculations Employing the Becke−Perdew Density Functional Approach

charge state	spin state	symm	property	$\epsilon = 1.0$	$\epsilon = 4.0$	$\epsilon = 10.0$	$\epsilon = 78.4$
4+ (IV, IV)	$S = 3$	C_{2h}	Mn−Mn distance/Å[a]	2.806	2.867	2.905	2.948
			O−O distance/Å[b]	2.371	2.454	2.490	2.517
			IE/eV[c]	23.41	7.52	4.31	2.51
5+ (IV, V)	$S = {}^5/_2$	C_s	Mn−Mn distance/Å[a]	2.888	2.869	2.885	2.908
			O−O distance/Å[b]	2.304	2.381	2.406	2.429
5+ (IV, V)	$S = {}^1/_2$	C_s	Mn−Mn distance/Å[a]	2.945	2.905	2.926	2.934
			O−O distance/Å[b]	2.271	2.377	2.416	2.445
			E_{rel}/kJ mol^{-1}[d]	4	14	0	3
5+ (IV, V)	$S = {}^3/_2$	C_s	Mn−Mn distance/Å[a]	2.932	2.904	2.922	2.938
			O−O distance/Å[b]	2.240	2.344	2.368	2.428
			E_{rel}/kJ mol^{-1}[d]	58	80	77	62

[a] Optimized distance between Mn atoms within the identified local minimum at the dielectric constant value (ϵ) indicated. [b] Optimized distance between bridging O atoms within the identified local minimum at the dielectric constant value (ϵ) indicated. [c] Ionization energy, in electronvolts (1 eV = 96.486 kJ mol^{-1}), at the dielectric constant value (ϵ) indicated. This quantity is the energy required to generate the $S = {}^5/_2$ $[Mn_2(\mu\text{-}O)_2(H_2O)_2(NH_3)_6]^{5+}$ species from the $S = 3$ +4 charge state structure. [d] Calculated total energy expressed relative to that of the $S = {}^5/_2$ +5 charge state local minimum at the dielectric constant value (ϵ) indicated.

ment (using $\epsilon = 78.4$),[14] but in this instance, the energy difference between the two identified geometries was only ~40 kJ mol^{-1}. A point of concern is that this solvent-field-corrected energy difference is small when compared against the uncertainties arising from the use of severely constrained complex geometries. (Adjustment of the Mn−O and O−O separations was not accompanied by any relaxation of the remaining components of the complex.)

To address this issue, we have used the COSMO[22−24] protocol implemented within ADF2002.[25] This model allows the incorporation of a solvent field in a manner comparable to that effected in the Gaussian 94 program suite used by ARA. Calculations employing alternatively the dielectric constant value $\epsilon = 78.4$ appropriate to water or the less severe values of $\epsilon = 4.0$ and 10.0, which are broadly representative of the range of condensed-phase corrections appropriate to a bulk protein environment,[35] were pursued toward two distinct goals. First, we performed full optimizations (within the dielectric field) of the lowest C_s-symmetry stationary points of spin states $S = {}^1/_2$, ${}^3/_2$, and ${}^5/_2$ for the +5 charge state to determine the viability of the vacuum-phase geometries for these species within a more realistic environment: results for $\epsilon = 4$, 10, and 78.4 are presented in Table 2 and discussed below. Second, we employed partially optimized (vacuum-phase) geometries for species of charge state +5, spin state $S = {}^7/_2$, C_{2h} symmetry, and with incrementally varied Mn−Mn separations (ranging from r(Mn−Mn) = 3.6 to 5.6 Å) to assess the solvent-corrected potential energy surface relating to O−O bond formation within, and O_2 loss from, the +5 charge state complex.

The field-corrected optimized geometries (summarized in Table 2) are not greatly different from those obtained through vacuum-phase ($\epsilon = 1$) calculations. The imposition of a dielectric environment leads to a generally negligible change in the Mn−Mn distance for the +5 charge state minima. The change seen for the O−O distance is more marked, with

(35) Schutz, C. N.; Warshel, A. *Proteins: Struct., Funct., Genet.* **2001**, *44*, 400.

consistent increases in this parameter for $\epsilon = 4$, 10, and 78.4 seen for each of the $S = {}^1/_2$, ${}^3/_2$, and ${}^5/_2$ spin states. This trend in the separation between bridging oxygen atoms strongly suggests that the stationary points located upon the +5 charge state are genuine minima that appear quite resistant to O−O bond formation. Relative energies for these three spin states are conserved fairly well across the four dielectric field strengths ($\epsilon = 1$, 4, 10, and 78.4) surveyed in our calculations, indicating that the surrounding environment likely has little effect on the magnetic properties of the dinuclear complex.

The comparison of the +5 charge state structural energetic values with that of the +4 charge state (represented in Table 2, for reasons of computational expediency, by the ferromagnetic $S = 3$, C_{2h}-symmetry minimum which lies approximately 30 kJ mol^{-1} higher in total energy than the broken-symmetry minimum for this charge state) is instructive. As shown in Table 2, the inclusion of a comparatively modest dielectric field ($\epsilon = 4$) is sufficient to reduce the energy separation between +4 and +5 charge-state species (that is, the ionization energy of the +4 charge state) from ∼23−24 to ∼7.5 eV, with further significant reductions when ϵ is ramped up to 10 and then to 78.4. This dramatic reduction in the energy separation between reduced and oxidized forms of the dinuclear complex is a forceful indication of the magnitude of the Coulombic stress against which our vacuum-phase +5 charge state geometries are nevertheless stable and an indication also of the perils in inferring from such vacuum-phase calculations the dissociative tendencies of multiply charged species under more realistic condensed-phase conditions.

Our solvent-corrected exploration of the dissociative tendencies of the +5 charge state structure is also very informative. Here, the $S = {}^7/_2$ spin state is investigated for two reasons: First, in our vacuum-phase calculations described in the preceding sections, the $S = {}^7/_2$ configuration was the only spin state found to lead to spontaneous dissociation of the dinuclear core. Second, this configuration disfavors a $Mn^{IV}Mn^{V}(O^{2-})_2$ electronic occupation because of the necessity to accommodate seven unpaired electrons. In contrast, feasible $Mn^{IV}Mn^{IV}(O_2{}^{3-})$, $Mn^{III}Mn^{IV}(O_2{}^{2-})$, $Mn^{III}Mn^{III}(O_2{}^{-})$, and $Mn^{II}Mn^{III}(O_2)$ occupations for the $S = {}^7/_2$ spin state can all be satisfactorily assigned; therefore, this spin state is expected to provide a useful diagnostic for the propensity of the +5 charge state to promote O−O bonding upon complex fragmentation: if the $S = {}^7/_2$ spin state, which is more electronically susceptible to oxo-bridge oxidation than the $S = {}^1/_2$ and ${}^5/_2$ spin states, is resistant to O_2 evolution then we can reasonably infer that $S = {}^1/_2$ and ${}^5/_2$ spin states are likely rather more resistant. Note that, for these calculations, we have used vacuum-phase partially optimized geometries within the solvent-field-corrected single-point calculations because of the very high demands on CPU time required for geometry optimization calculations involving COSMO corrections. However, the comparison of optimized geometries in Table 2 suggests that there should be comparatively little error introduced by the use of vacuum-phase, rather than solvent-corrected, geometries in the $\epsilon > 1$ calculations.

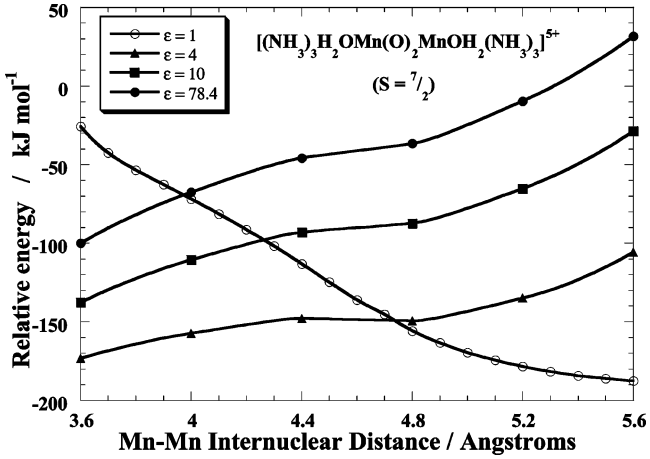

Figure 3. Comparison of vacuum-phase ($\epsilon = 1$) and condensed-phase ($\epsilon = 4$, 10, 78.4) potential energy curves for Mn−Mn elongation in the +5 charge state complex having C_{2h} symmetry and $S = {}^7/_2$. Geometries used in all constituent single-point calculations were those obtained from a BP/TZP relaxed linear transit calculation in the vacuum phase.

We find, when dielectric effects are included, that the energy profile seen for complex dissociation is effectively inverted (Figure 3). Even at our lowest solvent-field correction of $\epsilon = 4$, the attenuation of the Mn−Mn distance from 3.6 to 5.6 Å bears an energetic cost of ∼70 kJ mol^{-1}, implying a barrier to complex dissociation and O_2 release of at least this magnitude. Larger activation-energy lower limits of ∼110 and 130 kJ mol^{-1} are suggested by the $\epsilon =$ 10 and 78.4 scans, respectively.

A more reliable indication of the energetic requirements for +5 charge state complex dissociation may in fact be obtained by comparing the total calculated energies of the $S = {}^5/_2$ apparent global minimum on the dielectrically corrected PES and of the $S = {}^7/_2$ r(Mn−Mn) = 5.6 Å partially optimized geometry, which represents the highest point surveyed for the dissociative (O_2-releasing) pathway. For $\epsilon = 4$, these energies are respectively −7.104 and −6.971 hartrees (1 hartree = 2625.5 kJ mol^{-1}), demonstrating that the TS to dissociation (which we have not, of course, even reached in our scans) is at least 350 kJ mol^{-1} above the apparent +5 charge state global minimum. For $\epsilon = 10$ and 78.4, the corresponding energy elevation is at least 480 and 610 kJ mol^{-1}, respectively. These comparisons suggest that regardless of our uncertainty of the appropriate ϵ value within the protein environment the complex's dissociation in the condensed phase is a pathway of considerable energetic cost requiring substantial unfavorable concerted motion of the relevant structural fragments. According to our calculations, therefore, the $[(H_2O)(H_3N)_3Mn(\mu\text{-}O)_2Mn(NH_3)_3(OH_2)]^{n+}$ system cannot be considered a reliable model for the PSII active center.

Concluding Remarks

A recent theoretical study has suggested that the spontaneous dissociation and O_2 evolution of a di-μ-oxo bridged, dinuclear manganese complex in the +5 charge state is a model for the active features of the oxygen-evolving complex (OEC) within PSII. Our pure DFT calculations do not support

this suggestion. We find that, within the vacuum phase (which is intrinsically much less tolerant of compact highly charged molecular structures than the dielectrically blanketed environment of the condensed phase, whether solvated or within the bare protein), the +5 charge state of the identified Mn_2 complex possesses several local minima that correspond to metastable geometries of spin states $S = {}^1/_2$, ${}^3/_2$, and ${}^5/_2$. Only the $S = {}^7/_2$ configuration of the +5 charge state complex is found to dissociate spontaneously within the vacuum phase. Furthermore, even this instability is found to be rectified by the inclusion of a comparatively modest ($\epsilon = 4$) dielectric constant in COSMO solvent-field-corrected calculations, which suggest that within the condensed phase the +5 charge state dissociation and oxygen evolution are inhibited by a barrier of several electronvolts. We conclude that it is highly unlikely that the evolution of O_2 proceeds from two μ-oxo bridge atoms within a dinuclear Mn subunit of the OEC.

Acknowledgment. We gratefully acknowledge the Australian Research Council (ARC) for financial support.

Supporting Information Available: Cartesian coordinates for the $Mn_2O_2(H_2O)_2(NH_3)_6$ geometries encompassed in Table 1. This material is available free of charge via the Internet at http://pubs.acs.org.

IC049967K